DEVELOPMENT OF GPS CONSTELLATION POWER MONITOR SYSTEM FOR HIGH ACCURACY CALIBRATION/VALIDATION OF THE CYGNSS L1B DATA

Tianlin Wang[1], *Christopher Ruf*[1], *Scott Gleason*[2], *Bruce Block*[1], *Darren McKague*[1], *Damen Provost*[1]

[1]University of Michigan, Ann Arbor, MI USA [2]Southwest Research Institute, Boulder, CO USA

ABSTRACT

The Cyclone Global Navigation Satellite System (CYGNSS) uses the Global Positioning System (GPS) constellation (32 satellites) as the active source in a bi-static radar configuration, with CYGNSS acting as the passive radar receiver. A knowledge of Equivalent Isotropically Radiated Power (EIRP), based on transmit power and antenna pattern of GPS satellites, is of great importance in the accurate calibration of L1B data (bistatic radar cross section, BRCS) of the CYGNSS mission. However, the current knowledge of the EIRP of GPS satellites is limited. There exists an uncertainty of transmit power, and only 20 laboratory-measured antenna patterns have been published. Due to the azimuthal asymmetry of the patterns, the yaw attitude of GPS satellites may affect the EIRP. Therefore, a ground-based GPS constellation power monitor system has been built to accurately and precisely measure GPS signals in watts and, from that, estimate the transmit powers and antenna patterns of all GPS satellites. Measurement data without absolute calibration demonstrates that the GPS yaw attitude does affect the received power. A low noise amplifier (LNA) and calibration subsystem implemented on a PID controlled thermal plate is calibrated with a liquid nitrogen source, showing stable and reasonable results. With the absolute calibration of GPS signals. the retrieved GPS parameters will serve as inputs to the CYGNSS L1B calibration algorithm to improve the data accuracy.

Index Terms— CYGNSS, GPS constellation power monitor, calibration/validation, antenna pattern retrieval

1. INTRODUCTION

The Cyclone Global Navigation Satellite System (CYGNSS) is a space-borne mission to investigate the inner core processes of tropical cyclones. CYGNSS has two advantages: the capability to penetrate the eye wall and inner rain bands; the extremely short revisit time due to a dense constellation of microsatellites [1].

The CYGNSS mission was successfully launched on December 15th, 2016. The Level 1A calibration algorithm converts the Delay Doppler Maps (DDMs) from raw 'counts' to units of watts, and then the Level 1B calibration algorithm uses external metadata to convert the power in watts to BRCS and an effective scattering area [2]. The accuracy of data calibration and validation is very significant to the effectiveness of the science data products including the mean square slope and the wind speed.

To improve the accuracy of the CYGNSS L1B data product, a GPS constellation power monitor system has been designed, built, and calibrated at University of Michigan, Ann Arbor, to determine the EIRP of GPS signals. It is used to address three main factors: 1). uncertainty of GPS transmit power (approximately 25 watts); 2). azimuthal asymmetry in the published antenna patterns; 3). variations in the yaw attitude of the GPS satellites. The measurement data in Section 5 demonstrate that the satellite yaw attitude does affect the received power on the ground due to the pattern asymmetry.

The cold load, warm load, excess noise source, and LNAs are designed and implemented on a thermal plate with a PID temperature controller for absolute calibration. Using ground measurements and prior approximate knowledge of the GPS antenna patterns, the retrieved transmit powers and antenna patterns are derived. They will serve as inputs to the L1B calibration algorithm to improve the accuracy of calibrated BRCS products.

This paper is organized as follows. Section 2 introduces the physical model, antenna pattern asymmetry, and the retrieval algorithm. Section 3 presents the system design and hardware implementation. Section 4 is the data processing and software development. Section 5 compares the scaled model prediction and measurement data. Section 6 shows the diagram of radiometric calibration subsystem and results of liquid nitrogen calibration. Section 7 concludes the paper and introduces future work.

2. ELEMENTS OF THE METHOD AND SOLUTION

2.1. Physical Model

Based on the Friis transmission equation [5], the physical model is given by

$$\frac{P_R}{P_T} = \left(\frac{\lambda}{4\pi R}\right)^2 G_t(\theta_t, \phi_t) G_r(\theta_r, \phi_r) A\,(\theta_r) \quad (1)$$

where P_R and P_T are the received power and GPS transmit power, respectively; λ is the wavelength, R is the range; $G_t(\theta_t, \phi_t)$ and $G_r(\theta_r, \phi_r)$ are the gains of the transmit and receive antenna, respectively; $A\,(\theta_r)$ is atmospheric loss.

The velocity and position of GPS satellites in Earth-Centered, Earth-Fixed (ECEF) coordinates are computed by the GPS receiver, from which we calculate the range and elevation and azimuth angles.

The full antenna pattern of the receive antenna was measured by our colleagues at the ElectroScience Laboratory of the Ohio State University. The receiver gain is computed by importing the elevation and azimuth angles.

The attenuation of oxygen dominates the atmospheric loss in the GPS L1 band and the effects of water vapor, rain, and nitrogen attenuation are negligible [6]. Therefore, a simplified model is used to estimate the atmospheric loss factor, with dependence only on local elevation angle.

By using the GPS constellation power monitor system, we can measure all GPS signals in time-series. Absolute calibration enables us to determine the received signal's power in watts. The objective of this research is to retrieve the transmit power and the full 2D antenna pattern from the time-series received power.

2.2. The Antenna Pattern Asymmetry

The 20 GPS antenna patterns in [3] include: 8 'legacy' patterns for the first 8 of 12 classic IIR space vehicles (SVs);12 'improved' panel patterns for the final 4 of 12 classic IIR SVs; and all 8 of the modernized IIR-M SVs.

The IIR SV body axes are defined as: +Z axis directed toward Earth (nadir); +Y axis along the "positive" solar array axis; +X completes right-handed system [3].

The antenna pattern coordinates are defined by two angles: theta, θ, and phi, ϕ. θ is the angle across the face of the antenna panel from the +Y solar array ($\theta = -90°$), through the nadir direction ($\theta = 0°$), to the $-$Y solar array ($\theta = 90°$). ϕ is counter-clockwise around the antenna panel boresight (earth-facing) axis from 0° to 360°. $\phi = 0°$ refers to the SV +X axis [3]. The full 2D pattern extends θ from $-90°$ to 90° in 2° step, and ϕ from 0 to 360° in 10° step.

The Edge of Earth (EoE) boresight angle is defined as $\theta = \pm 13.8°$ for the GPS orbit, which defines the region of interest that provides terrestrial services. The azimuthally averaged patterns are plotted in Fig. 1. The improved antenna panel includes new antenna element designs and configurations to have increased power [3].

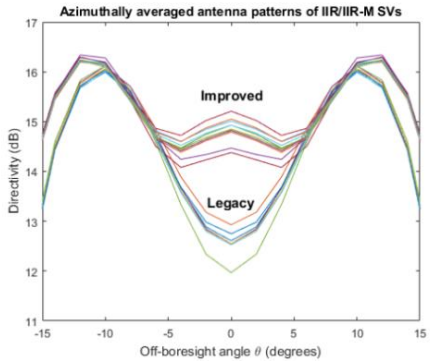

Fig. 1. Azimuthally averaged antenna patterns

The gain difference map of $\theta = 0{\sim}14°$ and $\phi = 0°{\sim}360°$ of GPS16 (PRN) are plotted in Fig. 2, which is of the difference between the true 2D antenna pattern and an azimuthally averaged pattern. We can observe the asymmetry for different values of ϕ. When $\theta = 14°$, the maximum and minimum difference values are 0.50 dB and -0.85 dB, respectively.

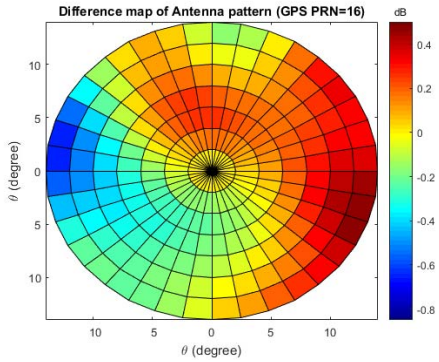

Fig. 2. Difference map of antenna pattern of GPS16

The standard deviations of the azimuth directivity vs. off-boresight angle θ for all IIR/IIR-M SVs are plotted in Fig. 3. Standard deviations over the range 5°~10° off-boresight angle are between 0.1 dB and 0.2 dB for most antenna patterns.

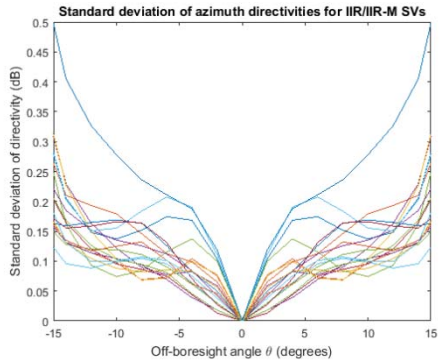

Fig. 3. Standard deviations of azimuth directivities

Due to the GPS satellites' yaw attitude variations [7], the around-boresight angle ϕ for the GPS SVs changes with the GPS attitude. This causes the gain of the transmit antenna to be dependent on satellite attitude.

2.3. Retrieval Algorithm

The retrieval algorithm is based on a minimum squared error estimator of the GPS transmitter parameters.

The state vector is defined as

$$\vec{x} = (c_0, c_1, c_2, c_3, c_4, c_5, P_{\mathrm{T}}) \quad (2)$$

which contains 6 coefficients in the 5th order polynomial model for the antenna pattern and the power P_{T}.

The data vector is defined as

$$\vec{y} = [y_1, y_2, \cdots, y_i, \cdots, y_N] \quad (3)$$

where y_i is the measurement made at time t_i.

The link model $f(\vec{x})$ estimates the received power at time t_i is given by

$$f_i(\vec{x}) = \left(\frac{\lambda}{4\pi R_i}\right)^2 G_r(\theta_{ri}, \phi_{ri}) A\,(\theta_{ri})[G_t(\theta_{ti}, \phi_{ti}) P_T\,] \quad (4)$$

where $[G_t(\theta_{ti}, \phi_{ti}) P_T\,]$ is a function of the state vector $\vec{x}$.

The model predictions for all measurements as function of the state vector are given by

$$\vec{F}(\vec{x}) = [\,f_1(\vec{x}), f_2(\vec{x}), \cdots, f_i(\vec{x}) \cdots, f_N(\vec{x})] \quad (5)$$

The minimum-squared-error solution for $\vec{x}$ is that value which minimizes squared difference between $\vec{y}$ and $\vec{F}(\vec{x})$

$$\vec{x}_{\mathrm{MSE}} = \min_{\vec{x}} \left\{ \left| \vec{y} - \vec{F}(\vec{x}) \right|^2 \right\} \quad (6)$$

Because model prediction $f(\vec{x})$ is a non-linear function of the components of $\vec{x}$, then $\vec{x}_{\mathrm{MSE}}$ is estimated iteratively.

Let $\vec{x}_j$ be the j^{th} estimate of the state vector $\vec{x}$, then the $(j+1)^{\mathrm{th}}$ estimate $\vec{x}_{j+1}$ can be computed by

$$\vec{x}_{j+1} = \vec{x}_j + \left(\bar{\bar{J}}^T \bar{\bar{J}}\right)^{-1} \bar{\bar{J}}^T \left[\vec{y} - \vec{F}(\vec{x}_j)\right] \quad (7)$$

where $\bar{\bar{J}}$ is the Jacobian matrix of $\vec{F}(\vec{x}_j)$.

In practice, a first guess at $\vec{x}$ is made and then Equation (7) is iterated until changes in $\vec{x}$ become acceptably small. In this problem, the initial guess for components of $\vec{x}$ is $P_{\mathrm{T}} = 25\,Watts$ and, for the polynomial coefficients, a 5th order curve fitting of azimuthally averaged antenna patterns provided by Lockheed Martin [3].

3. SYSTEM DESIGN AND IMPEMENTATION

The GPS constellation power monitor system was designed and built at Space Physics Research Laboratory, University of Michigan, Ann Arbor. As shown in Fig. 4, a mast-mounted, passive Javad RingAnt-DM antenna with a surge protector is set on the roof of the Space Research Building ($42.29412°\,\mathrm{N}$, $83.711391°\,\mathrm{W}$) to receive the GPS L1 signal. Elevation mask is 20° to filter out multipath signal.

(a). Location (b). Side view

Fig. 4. Javad RingAnt-DM antenna

The signal is filtered by two GPS bandpass filters with 50 MHz and 5 MHz bandwidth centered at 1.57542 GHz. Cold load, ambient load, and noise source are integrated onto a thermal baseplate, where the temperature is actively controlled by a PID controller. The thermal plate is set to a constant temperature to keep the LNA and isolators at a stable gain and self emission. The signal is then sent to the Septentrio PolaRxS receiver to generate the binary data files. A picture of the LNA and calibration subsystem is shown in Fig. 5.

The calibration subsystem is described in Section 6.

Fig. 5. LNA and calibration subsystem implemented on the PID controlled thermal plate

4. DATA PROCESSING AND SOFTWARE

The measurement data include the following significant information: the position and the velocity, the azimuth and elevation angles, and the received power in the form of the real and imaginary post-correlation values, I and Q.

The exact power in watts is proportional to I^2+Q^2. Before the absolute calibration, a scaling factor is introduced to match the model simulation (units: watts) and the measurement data (arbitrary unit, AU).

The data used in the Section 5 were measured before the implementation of the GPS bandpass filters. Therefore a moving average is applied to filter low frequency noise.

The GPS constellation yaw attitude will be imported from the GNSS-Inferred Positioning System and Orbit Analysis Simulation (GIPSY-OASIS) by NASA-JPL.

5. SIMULATION AND MEASUREMENT RESULTS

Measurements were performed on 15 August 2016. Data are moving averaged by 100 seconds to filter the noise. The elevation angle (red) and the I^2+Q^2 values (blue) are shown in Fig. 6. The maximum elevation angle is 88.81 degrees.

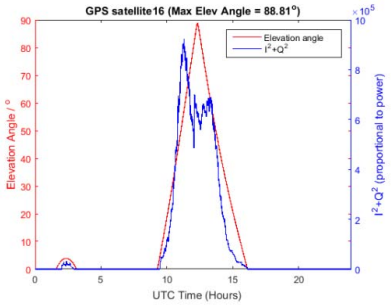

Fig. 6. The elevation angles and I^2+Q^2 values of measurement

It should be noted this measurement was taken before implementation of the thermal plate. The peak in the measured signal is likely caused by a gain change of the LNA due to the rapid temperature change at sunrise (Local ~7:30 AM).

The model prediction of power in watts is scaled by a multiplicative factor to be close to the I^2+Q^2 values. In Fig. 7, the measurement (black), the simulation using the

measured ϕ (red), and the simulation using the corrected ϕ with a specific rotation (blue) are compared. ϕ is the around-boresight angle defined in Section 2.2. We find that the mismatch between initial model prediction and measurement can be corrected by the rotation of ϕ. This demonstrates that the GPS satellite yaw attitude does affect the gain of transmit antenna due to the pattern asymmetry.

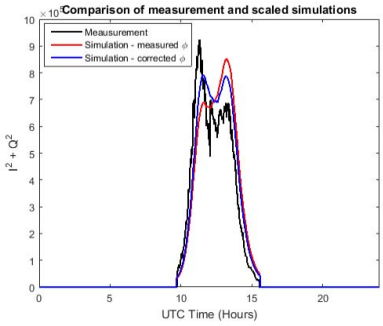

Fig. 7. The comparison of measurement and scaled simulations

6. RADIOMETRIC CALIBRATION

To calibrate the GPS signals' power in watts, the internal noise sources are located in a calibration subsystem with the LNA and attached to a thermal plate. Liquid nitrogen calibration is performed before deployment to calibrate the brightness temperature of the internal noise sources.

A diagram of the radiometric calibration is shown in Fig.8. The objective is to calibrate the brightness temperature, TB, of the internal cold load and the noise diode by using an external liquid nitrogen load and the internal ambient load as references. The RF output is connected to a Septentrio receiver, with AGC mode turned off and the gain manually set to 32 dB.

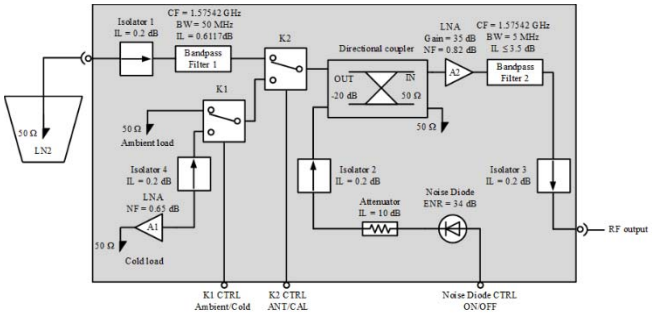

Fig. 8. Radiometric calibration diagram

Fig. 9 shows the time-series averaged power measured by the Septentrio receiver. There are 6 measurement states: External LN2 Start, Internal Cold, Internal Cold + Noise Diode, Internal Ambient, Internal Ambient + Noise Diode, and External LN2 End. In a single routine, each state is measured for 0.5 hour. One calibration routine gives 3 hours' data. The liquid nitrogen calibration is repeated three times, giving totally 9 hours' data. The averaged powers of all 6 states are stable. The TB of liquid nitrogen is 80.5K, and the equivalent TB of the LN2 load at K2 is 120.8K. The calibrated TB of the cold load is 59.4K. The calibrated TB of the noise diode is 110.9K by $TB_{\text{Ambient+ND}} - TB_{\text{Ambient}}$ and 110.2K by $TB_{\text{Cold+ND}} - TB_{\text{Cold}}$, which are reasonable and will be used for absolute calibration of GPS signals.

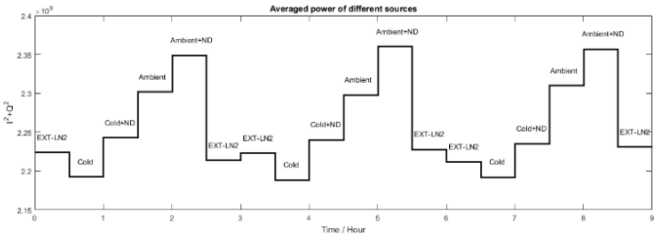

Fig. 9. The averaged powers of different sources

7. CONCLUSION AND FUTURE WORK

A GPS constellation power monitor system has been designed, built and operated to estimate the transmit power and antenna pattern of each GPS satellite and to determine the EIRP of GPS signals. The objectives are to broaden our knowledge of GPS sources and to improve the accuracy of the L1B data of the CYGNSS mission.

From the measurement without absolute calibration, we have demonstrated that the GPS satellite yaw attitude does affect the received power due to the antenna pattern asymmetry. The calibration subsystem is implemented on a PID controlled thermal plate and has been radiometrically calibrated through a standard liquid nitrogen calibration process, showing stable and reasonable results.

Future work will include the absolute calibration of received GPS signal's power in watts, accurate retrieval of the GPS transmit powers and antenna patterns, and high accuracy calibration of the L1B BRCS data of the CYGNSS mission.

8. REFERENCES

[1] C. S. Ruf, A. Lyons, M. Unwin, J. Dickinson, R. Rose, D. Rose, and M. Vincent, "CYGNSS: Enabling the Future of Hurricane Prediction," *IEEE Geosci. Remote Sens. Mag.*, vol. 1, no. 2, pp. 52-67, June 2013.

[2] Ruf, C. S., et al, *CYGNSS Handbook*, Michigan Publishing, Ann Arbor, MI, 2016.

[3] W. A. Marquis and D. L. Reigh, "The GPS Block IIR and IIR-M Broadcast L-band Antenna Panel: Its Pattern and Performance," *Navigation*, vol. 62, no. 4, pp. 329-347, Dec 2015.

[4] S. Gleason, C. S. Ruf, M. P. Clarizia, and A. J. O'Brien, "Calibration and Unwrapping of the Normalized Scattering Cross Section for the Cyclone Global Navigation Satellite System," *IEEE Trans. Geosci. Remote Sens.*, vol. 54, no. 5, pp. 2495-2509, May 2016.

[5] Ulaby, F. T., et al, *Microwave Radar and Radiometric Remote Sensing*, University of Michigan Press, Ann Arbor, MI, 2014.

[6] Parkinson, B. W., and J. J. Spilker, *Global Positioning System: Theory and Applications*, American Institute of Aeronautics and Astronautics, Washington, DC, 1996.

[7] Y. E. Bar-Sever, "A New Model for GPS Yaw Attitude," *Journal of Geodesy,* vol. 70, no.11, pp. 714-723, Nov. 1996.